Cross-symmetric dipolar-matter-wave solitons in double-well chains

Zhiwei Fan,[1] Yuhan Shi,[1] Yan Liu,[1,*] Wei Pang,[2] Yongyao Li,[1,3,†] and Boris A. Malomed[1,4,5]

[1]*Department of Applied Physics, South China Agricultural University, Guangzhou 510642, China*

[2]*Department of Experiment Teaching, Guangdong University of Technology, Guangzhou 510006, China*

[3]*School of Physics and Optoelectronic Engineering, Foshan University, Foshan 528000, China*

[4]*Department of Physical Electronics, School of Electrical Engineering, Faculty of Engineering, Tel Aviv University,*
Tel Aviv 69978, Israel

[5]*Laboratory of Nonlinear-Optical Informatics, ITMO University, St. Petersburg 197101, Russia*

We consider a dipolar Bose-Einstein condensate trapped in an array of two-well systems with an arbitrary orientation of the dipoles relative to the system's axis. The system can be built as a chain of local traps sliced into two parallel lattices by a repelling laser sheet. It is modeled by a pair of coupled discrete Gross-Pitaevskii equations, with dipole-dipole self-interactions and cross interactions. When the dipoles are not polarized perpendicular or parallel to the lattice, the cross interaction is asymmetric, replacing the familiar symmetric two-component discrete solitons by two new species of cross-symmetric ones, viz., on-site- and off-site-centered solitons, which are strongly affected by the orientation of the dipoles and separation between the parallel lattices. A very narrow region of intermediate asymmetric discrete solitons is found at the boundary between the on- and off-site families. Two different types of solitons in the $\mathcal{PT}$-symmetric version of the system are constructed too, and stability areas are identified for them.

I. INTRODUCTION

Bose-Einstein condensates (BECs) composed of dipolar atoms and molecules are a broad research area in low-temperature physics. This type of BEC, dominated by anisotropic long-range magnetic or electric dipole-dipole interactions (DDIs), is significantly different from usual condensates, whose intrinsic dynamics is determined by point-blank interatomic collisions. Studies of dipolar BECs have produced a large number of specific experimental and theoretical results, which have been summarized in Refs. [1–3].

In addition to the fact that the atomic or molecular dipoles can be polarized by external dc electric or magnetic fields, the sign of the DDI can be switched by the ac rotating field [4]. These features lend dipolar BECs a great deal of tunability. In addition to the use of atoms or molecules carrying permanent magnetic or electric moments, condensates can be made of particles with dipole moments locally induced by the same dc fields, which polarize the moments, the latter setting with spatially nonuniform fields being especially interesting [5]. These properties enhance the potential offered by dipolar BECs for fundamental and applied studies. One significant direction in these studies is the use of dipolar condensates for emulation of various phenomena that occur in a more complex form in other physical media, such as rotons [6], ferrofluidity [7,8], Faraday waves [9], supersolids [10], anisotropic superfluidity [11], anisotropic collapse [12], mesoscopic droplets stabilized by quantum fluctuations [13], spin-orbit coupling in dipolar media [14], and others [15–18].

Another noteworthy ramification is the use of collective nonlinear modes in dipolar BECs for the creation of solitons in nonlocal media. This topic was originally introduced in optics,

where nonlocal nonlinearities of other types occur [19,20]. Various forms of bright [21], dark [22], vortex [23], and discrete [24] solitons were predicted in dipolar condensates. Recently, stable two-dimensional solitons were predicted in the dipolar BEC with spin-orbit coupling [25]. In addition to BECs, it was demonstrated that the DDI can create solitons in the ultracold bosonic gas of the Tonks-Gigardeau type [26].

A specific phenomenon that can be realized in dipolar BECs is the spontaneous symmetry breaking (SSB), and the related phase transition, alias the symmetry-breaking bifurcation, of modes created by such long-range anisotropic interactions. The SSB is a ubiquitous effect, which occurs in all areas of nonlinear physics [27]. Because the nonlinearity often creates solitons, a natural subject of the analysis is the SSB of solitons in symmetric systems. In particular, many theoretical and experimental results on this subject have been reported in photonic and matter-wave settings, where the nonlinearity is an inherent feature, and symmetry is frequently provided by dual-core or double-well structures [28]. The SSB for solitons in systems with local nonlinearity has been studied in detail theoretically [29–46], including discrete systems, which represent parallel arrays of coupled waveguides [47]. The study of the SSB for solitons in systems with nonlocal interactions is a problem of considerable interest too, as the nonlocality strongly affects the outcome of the competition between the nonlinear self-focusing of the fields and linear mixing between them, which leads to the SSB when the nonlinearity strength exceeds a critical value [28]. Thus far, only few works have addressed this topic. In particular, the SSB transformation of solitons in the dual-core coupler with nonlocal optical nonlinearity of the thermal type was considered in Ref. [48]. Unlike the optical systems, dipolar BECs feature not only the intracore nonlocal nonlinearity, but also the intercore DDI, which makes the situation essentially

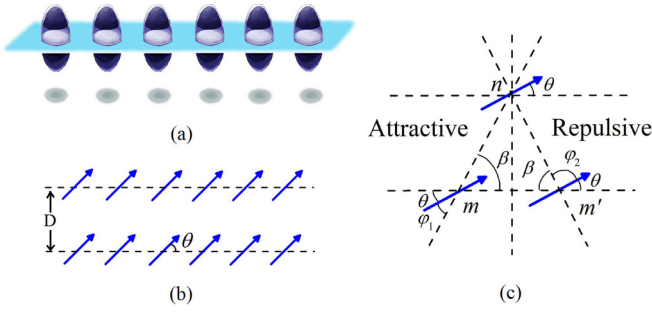*lycalm@scau.edu.cn
†yongyaoli@gmail.com

FIG. 1. (a) The system: a chain of tunnel-coupled traps for BEC, sliced by a repelling laser sheet into a stack of double wells, i.e., a pair of parallel lattices. (b) The orientation of dipoles in the system. D is the distance between the parallel lattices. (c) A typical example of the setting for the asymmetric nonlocal cross interaction. In this case, the $m \leftrightarrow n$ and $m' \leftrightarrow n$ DDI is attractive and repulsive, respectively, at $\varphi_1 < 54.7°$ and $\varphi_2 > 54.7°$.

different, as was first shown in the model for the effectively one-dimensional (1D) dual-core coupler filled by the dipolar condensate [49]. In that work, different types of SSB, sub-critical and supercritical ones (i.e., symmetry-breaking phase transitions of the first and second kinds, respectively) were demonstrated, as the result of the competition of the DDIs with strong or weak hopping between the cores. However, the analysis was performed in Ref. [49] only for a single polarization of the dipoles, namely, along the cores. However, the external magnetic field can polarize the dipoles in any direction; once the dipoles are not parallel or perpendicular to the core, nonlocal cross interaction induced by the DDIs becomes asymmetric, breaking the usual type of the solitons' symmetry.

The aim of the present work is to explore what kind of symmetry may be featured by two-component discrete solitons for oblique orientation of the dipoles. We demonstrate that, unless the dipole moments are oriented strictly perpendicular or parallel to the system's axis, the solitons' shapes become uneven (spatially asymmetric), which makes it necessary to modify the definition of the symmetry between the soliton's components, replacing it by cross symmetry. Actually, two types of cross symmetry are found for different sets of the system's parameters, see Eqs. (9) and (11) below. Here we study discrete solitons with such types of the symmetry.
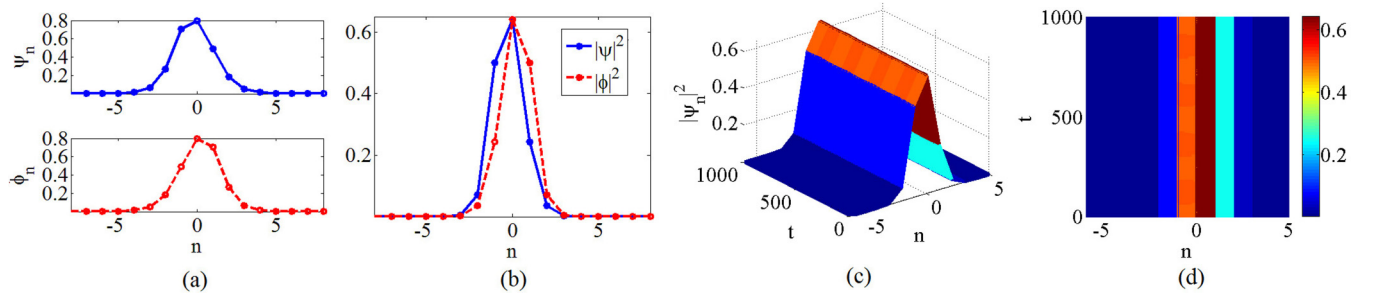
The rest of the paper is structured as follows. The two-component discrete model is introduced in Sec. II, and the cross symmetry of solitons in it, controlled by the orientation of the dipoles, is studied in Sec. III. In Sec. IV, we introduce a further generalization of the system, by lending it the $\mathcal{PT}$ symmetry (represented by spatially separated and mutually balanced gain and loss). The paper is concluded by Sec. V.

II. MODEL

We consider a chain of two-well systems, into which the dipolar BEC is loaded, as schematically shown in Fig. 1(a). It can be built as the usual quasi-one-dimensional lattice [50], split into a pair of parallel ones by an additional repulsive (blue-detuned) laser sheet. We consider configurations with different angles θ of the orientation of the dipoles with respect to the lattice, as shown in Fig. 1(b).

In the tight-binding approximation [51,52], the mean-field dynamics of the condensate in this system is governed by the two-component discrete Gross-Pitaevskii equation for wave functions $\tilde{\psi}_n$ and $\tilde{\phi}_n$ of particles trapped in local potential wells:

$$
\begin{aligned}
i\frac{d}{dt}\tilde{\psi}_n = &-\frac{C}{2}(\tilde{\psi}_{n+1} + \tilde{\psi}_{n-1}) \\
&+ \left[\sigma|\tilde{\psi}_n|^2 + \sum_{m \neq n}(F_{nm}|\tilde{\psi}_m|^2 + G_{nm}|\tilde{\phi}_m|^2)\right] \\
&\times \tilde{\psi}_n - J\tilde{\phi}_n, \\
i\frac{d}{dt}\tilde{\phi}_n = &-\frac{C}{2}(\tilde{\phi}_{n+1} + \tilde{\phi}_{n-1}) \\
&+ \left[\sigma|\tilde{\phi}_n|^2 + \sum_{m \neq n}(F_{nm}|\tilde{\phi}_m|^2 + G_{mn}|\tilde{\psi}_m|^2)\right] \\
&\times \tilde{\phi}_n - J\tilde{\psi}_n.
\end{aligned}
\tag{1}
$$

Here, C and J are, respectively, the coupling constants (determined by the respective hopping rates) along the lattice and between the parallel ones, σ is the strength of the contact nonlinearity, while F_{nm} and G_{nm} are DDI kernels, which account, severally, for the nonlocal self-interactions and cross interactions in the coupled Gross-Pitaevskii
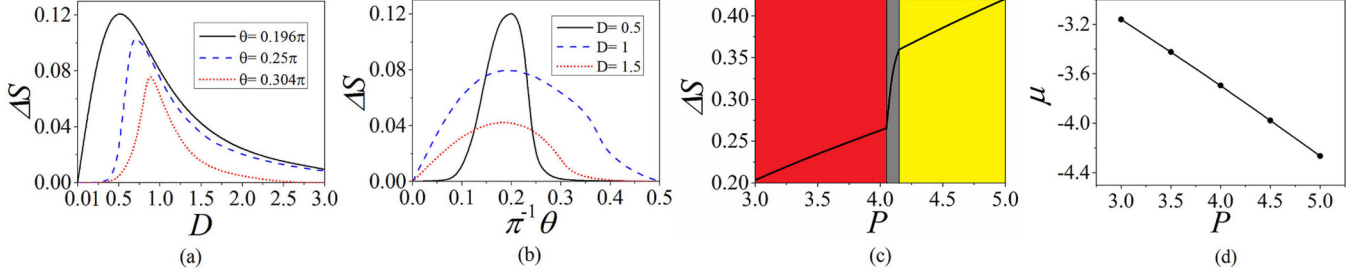

FIG. 2. A typical example of a cross-symmetric soliton for $(P,D,\theta) = (3,0.4,0.196\pi)$. (a) Shapes of two components of the solitons. (b) Juxtaposition of their density profiles. The blue and red curves are mirror images of each other. (c) Simulations of weakly perturbed evolution of the cross-symmetric soliton, which makes its stability evident. (d) A top view of the configuration displayed in (c).

FIG. 3. (a), (b) The cross-symmetry measure ΔS, defined as per Eq. (10), versus D and θ for discrete solitons featuring the cross symmetry of the on-site type, at a fixed total power, $P = 1.9$. (c) ΔS versus P (black solid curve) when $D = 0.5$ and $\theta = 0.196\pi$. Here, the line $\Delta S(P)$ traverses areas populated by three types of the discrete solitons: on-site cross-symmetric (red), intermediate state (gray), and off-site cross-symmetric (the yellow area). (d) Dependence $\mu(P)$ for $D = 0.5$ and $\theta = 0.196\pi$, which clearly satisfies the Vakhitov-Kolokolov (VK) criterion, $d\mu/dP < 0$.

equations:

$$F_{nm} = \begin{cases} 0, & (m = n) \\ (1 - 3\cos^2\theta)/|m - n|^3 & (m \neq n) \end{cases}, \quad (2)$$

$$G_{nm} = \begin{cases} (1 - 3\sin^2\theta)/D^3 & (m = n) \\ [1 - 3\cos^2\varphi_1]/[D^2 + (m - n)^2]^{3/2} & (m < n), \\ [1 - 3\cos^2\varphi_2]/[D^2 + (m - n)^2]^{3/2} & (m > n) \end{cases} \quad (3)$$

where D is the scaled separation between the parallel lattices, $\varphi_1 = \beta - \theta$, and $\varphi_2 = \pi - (\beta + \theta)$ [see in Fig. 1(c)], with $\beta \equiv \arccos(|m - n|/\sqrt{D^2 + (m - n)^2})$. Recently, a similar configuration was considered as an Ising model with long-range interactions, which does not include the transverse hopping, i.e., with $C = 0$ [53].

Stationary states are looked for in the usual form,

$$(\tilde{\psi}_n, \tilde{\phi}_n) = (\psi_n, \phi_n)e^{-i\mu t}, \quad (4)$$

where (ψ_n, ϕ_n) are stationary wave functions, and μ is a real chemical potential. Two-component solitons are characterized by their total norm,

$$P = P_\psi + P_\phi \equiv \sum_{n=-N/2}^{n=N/2} (|\tilde{\psi}_n|^2 + |\tilde{\phi}_n|^2), \quad (5)$$

which is a dynamical invariant of Eq. (1).

For $\theta = 0$ or $\pi/2$, matrix G_{nm} given by Eq. (3) is symmetric, with $G_{nm} = G_{mn}$. When $0 < \theta < \pi/2$, this property is broken, which makes nonlocal cross interaction asymmetric, see

Fig. 1(c). Obviously, at $\theta = 0$ vertical (alias interlattice) interactions, i.e., the onsite DDI between condensate droplets trapped in the two potential wells belonging to the parallel lattices, is repulsive, while the horizontal DDI along each lattice is attractive. With the increase of θ, the vertical interaction vanishes at

$$\theta_1 = \arcsin(1/\sqrt{3}) \approx 0.196\pi \approx 35.3° \quad (6)$$

while the horizontal DDI remains attractive. Another special angle,

$$\theta_2 = \arccos(1/\sqrt{3}) \approx 0.304\pi \approx 54.7°, \quad (7)$$

corresponds to the vanishing of the horizontal interaction, while the vertical DDI is attractive.

Obviously, at $\theta = 0$ and $\pi/2$, symmetric discrete solitons obey the spatial-symmetry condition,

$$\phi_{-n} = \phi_n, \quad \psi_{-n} = \psi_n. \quad (8)$$

However, when θ is different from 0 and $\pi/2$, shapes of the two components are not spatially even because, as mentioned above, G_{nm} is not a symmetric matrix anymore. In the following section we introduce another type of symmetry, which two-component discrete solitons may feature in this case. Here we present the asymmetric cross interactions corresponding to asymmetric G_{nm}.

III. CROSS-SYMMETRIC SOLITONS

To focus on effects induced by the DDIs, we drop the contact nonlinearity in the system, by setting $\sigma = 0$ in
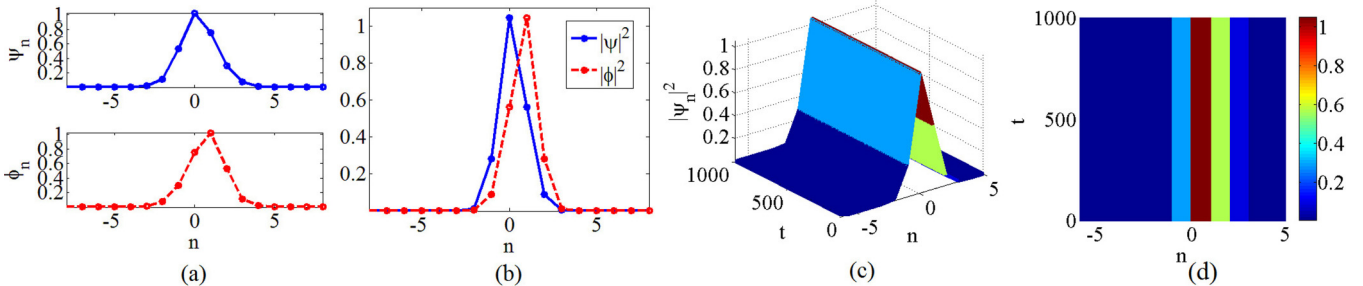

FIG. 4. A typical example of discrete solitons featuring the cross symmetry of the off-site type, see Eq. (11), for $(P, D, \theta) = (4, 0.4, 0.196\pi)$. Panels have the same meaning as in Fig. 2.
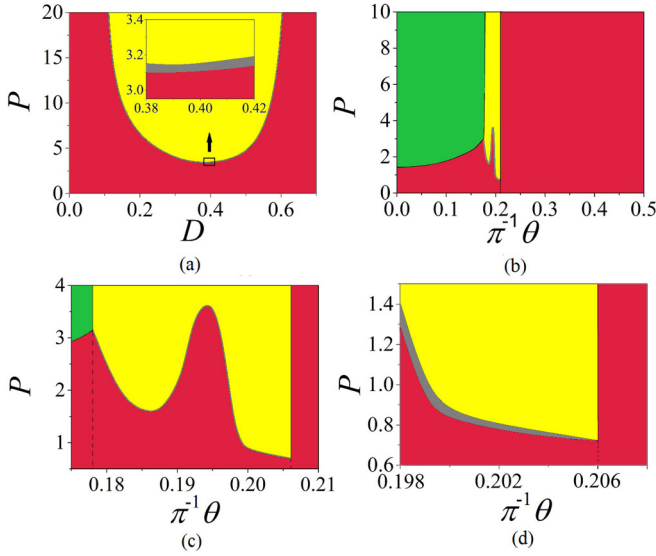
FIG. 5. Existence regions of stable discrete cross-symmetric discrete solitons of the on- and off-site are shown in parameter planes by red and yellow colors, respectively. In (a), orientation $\theta = 0.196\pi$ is fixed, and the off-site (yellow) area exists between $D = 0.1$ and 0.62. The inset in (a) displays a zoom around $D = 0.4$, with the minuscule gray area representing the intermediate state. In (b), $D = 0.4$ is fixed. In the green region, asymmetric solitons are found. The off-site solitons exist in the region between $\theta = 0.177\pi$ and 0.206π, which is displayed at a larger scale in (c). (d) is a zoom of a very small gray area, where the intermediate solitons are found at $0.198\pi < \theta < 0.206\pi$.

Eq. (1), and assume equal horizontal and vertical hopping rates, scaling both to be unity: $C = J = 1$. The remaining control parameters are P, D, and θ, i.e., the total norm of the solitons [see Eq. (5)], separation between the lattices, and the orientation of the dipoles, respectively. Here, we consider the case of $0 < \theta < \pi/2$, in which G_{nm} is not symmetric, as said above.

The only feasible approach to the study of the present system may be based on numerical methods. Discrete solitons in models with nearest-neighbor interactions can be explored by means of a variational approximation [54]; however, it cannot be developed in an analytically tractable form for lattices with long-range interactions.

Figure 2 displays a typical example of a two-component discrete soliton, with $(P, D, \theta) = (3, 0.4, 0.196\pi)$, obtained

numerically by means of the imaginary-time method [55–57]. The figure corroborates that the two components of the soliton indeed do not obey symmetry conditions (8); nevertheless, they satisfy the definition of the cross symmetry:

$$\phi_n = \psi_{-n}, \quad \psi_n = \phi_{-n}, \tag{9}$$

which is compatible with Eq. (1) in the case of asymmetric cross-interaction matrix G_{nm}. Note that locations of maxima of both components coincide in Fig. 2.

It is relevant to stress that all the soliton families considered below, which may be characterized by the respective dependences $\mu(P)$, satisfy the well-known Vakhitov-Kolokolov (VK) criterion [58], $d\mu/dP < 0$ [a typical example of dependence $\mu(P)$ is displayed in Fig. 3(d)], which is a necessary condition for stability of solitons against small perturbations. While this criterion was originally established for solitons in continuum media [58], its generalization for two-component discrete solitons is known too [59]. In fact, the results reported below demonstrate that the VK criterion is sufficient for the stability of discrete solitons in the present system (except for its $\mathcal{PT}$-symmetric extension, which is introduced in Sec. IV). In this connection, it is relevant to mention that, although configurations with dipoles oriented perpendicular to the system's direction tend to be the most stable [60], we here demonstrate that the discrete solitons with oblique orientations are stable too.

It follows from Eq. (9) that cross-symmetric solitons have equal norms of their components, $P_\psi = P_\phi$. The cross symmetry is quantified by the on-site mismatch between the components, defined as

$$\Delta S = \frac{1}{P} \sum_{n=-N/2}^{n=N/2} |(|\psi_n|^2 - |\phi_n|^2)|. \tag{10}$$

For usual symmetric solitons Eq. (10) yields $\Delta S = 0$, as it follows from Eq. (8). A larger magnitude of ΔS corresponds to a stronger mismatch between the two components.

The cross symmetry may suffer spontaneous breaking, similar to the above-mentioned SSB phenomena. This effect will be signaled by emergence of soliton solutions with $P_\psi \neq P_\phi$, and will be considered elsewhere.

The dependence of the cross-symmetry degree Eq. (10) on the interlattice separation D and orientation θ is displayed in Fig. 3, which shows that ΔS attains a maximum at finite values of D and θ. According to the figure, the cross symmetry is well pronounced around the maximum, in parameter
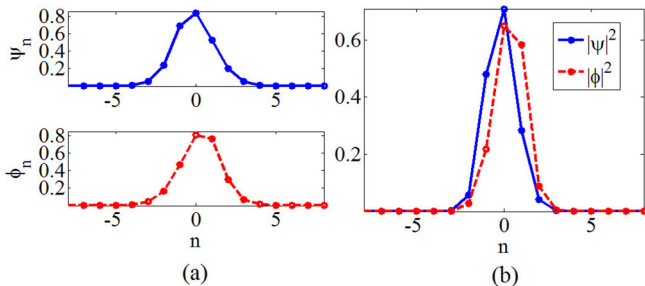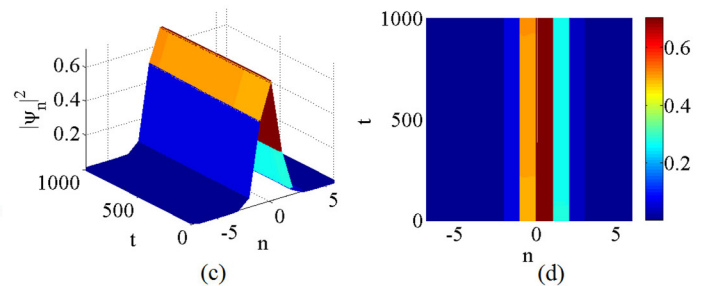

FIG. 6. A typical example of a stable asymmetric discrete soliton, intermediate between cross-symmetric ones of the on- and off-site types, for $(P, D, \theta) = (3.15, 0.4, 0.196\pi)$. Panels have the same meaning as in Figs. 2 and 4.
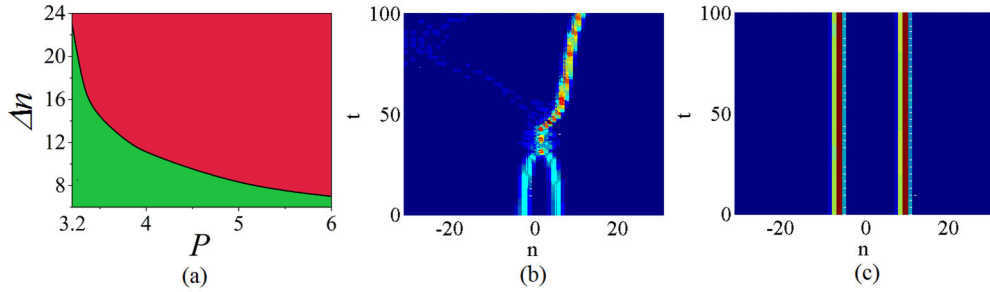
FIG. 7. (a) In the green area of the plane of $(P, \Delta n)$, two in-phase solitons with identical powers P, separated by initial distance Δn, merge into a single excited mode [as shown in (b) for $P = 4, \Delta n = 8$], while in the red area the solitons stay put [see (c), for $P = 4, \Delta n = 16$]. Other parameters are $D = 0.4, \theta = 0.196\pi$.

intervals $0.35 < D < 0.55$ and $0.18\pi < \theta < 0.22\pi$. Further consideration of solitons in this area with the increase of the total norm reveals another variety of the cross symmetry, different from that defined by Eq. (9). A typical example of the new variety is displayed in Fig. 4. Comparing it with the counterpart displayed above in Fig. 2, we find that maxima of the two components are separated in Fig. 4 by one lattice site, with the respectively modified cross symmetry defined as

$$\phi_n = \psi_{1-n}, \quad \psi_n = \phi_{1-n}, \quad (11)$$

cf. Eq. (9). It is possible to say that cross-symmetry axes, corresponding to definitions (9) and (11), are set, severally, on-site and off-site (at the midpoint between two sites in the latter case), therefore we refer to these two varieties as on- and off-site cross symmetries, respectively.

Existence areas of the cross-symmetric discrete solitons of these two types in the (P, D) and (P, θ) planes are displayed in Fig. 5, which shows that the off-site cross-symmetric solitons exist in finite areas [their boundaries are vertical in Figs. 5(b)–5(d) up to the accuracy of the numerical results]. Along the border between these areas, there is a very narrow band, shown as a gray strip, which is filled by discrete solitons of an intermediate type. They do not feature any explicit symmetry, except for the equality between the total norms of the two components, $P_\psi = P_\phi$, see a typical example in Fig. 6. The asymmetric intermediate states account for a continuous transition between the cross-symmetric discrete solitons of the on- and off-site types, being as stable as their cross-symmetric counterparts are. The continuity of the transition is made evident in Fig. 3(c) by the dependence of the cross-symmetry degree, ΔS [defined by Eq. (10)], on the total norm, going

across areas occupied by these three types of the discrete solitons.

We have also studied interaction between two cross-symmetric solitons, originally separated by distance Δn. If Δn is smaller than a certain critical value, $(\Delta n)_{cr}$, which corresponds to the boundary between green and red areas in Fig. 7(a), the solitons with zero phase shift between them attract each other and merge into a single excited (oscillating) state, as shown in Fig. 7(b). At $\Delta n > (\Delta n)_{cr}$, the pinning force from the underlying lattice is stronger than the attraction, and the solitons stay in the initial positions [see Fig. 7(c)]. It is easy to understand why $(\Delta n)_{cr}$ strongly grows with the decrease of P, as seen in Fig. 7(a): for small P, the broad solitons are quasicontinuum modes, for which the force of pinning to the lattice is exponentially small [61].

IV. TWO-COMPONENT DISCRETE SOLITONS IN THE SYSTEM WITH CROSS-$\mathcal{PT}$ SYMMETRY

Theoretical studies of many linear- and nonlinear-wave systems may be naturally extended by adding the $\mathcal{PT}$ symmetry, i.e., spatially symmetric distributions of globally balanced gain and loss terms [62,63]. In particular, much interest has been drawn to solitons in $\mathcal{PT}$-symmetric systems [64]. In term of matter waves, the gain and loss represent symmetrically placed and mutually balanced sources and sinks of coherent atoms. Although the experimental realization of sources in BECs may not be easy, the theoretical analysis of BEC-$\mathcal{PT}$ systems has attracted considerable interest, see, e.g., Refs. [65–68]. In particular, a model applying the $\mathcal{PT}$ symmetry to dipolar BECs trapped in a symmetric double-potential well was
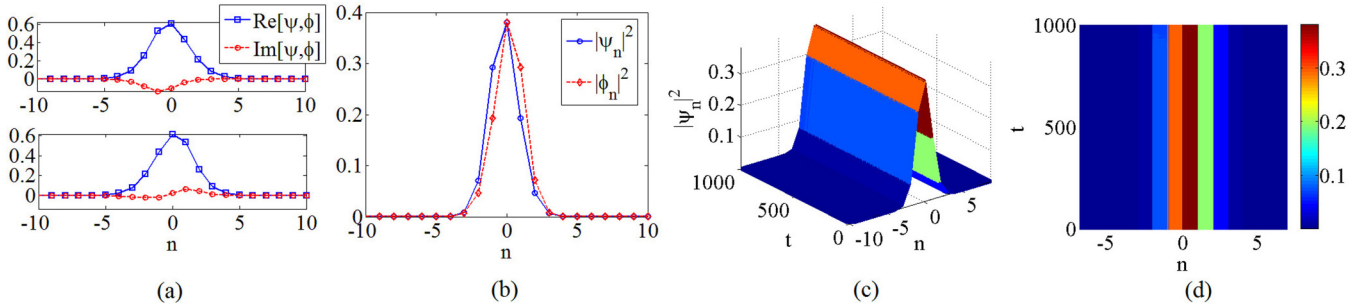

FIG. 8. A typical example of stable cross-$\mathcal{PT}$-symmetric solitons of the on-site type, for $(P, D, \theta, \kappa) = (2, 0.4, 0.196\pi, 0.2)$. (a) displays the real and imaginary parts of both field components. (b), (c), and (d) have the same meaning as in Figs. 2, 4, and 6.
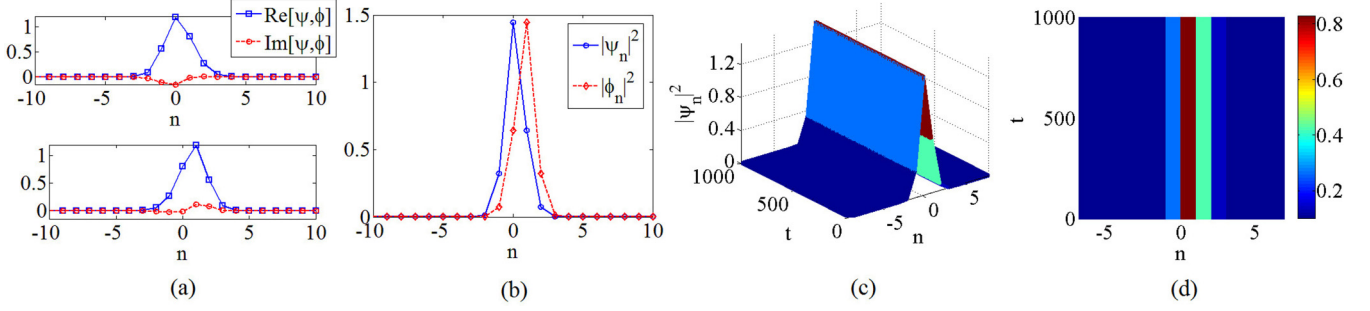
FIG. 9. A typical example of stable cross-$\mathcal{PT}$-symmetric solitons of the off-site type, for $(P,D,\theta,\kappa) = (5,0.4,0.196\pi,0.1)$. Panels have the same meaning as in Fig. 8.

proposed recently [69]. In this section, we aim to develop the $\mathcal{PT}$-symmetric version of the system based on Eq. (1), which, in particular, will provide an example of a discrete $\mathcal{PT}$-symmetric system with long-range interactions.

Thus, Eq. (1) is replaced by

$$i\frac{d}{dt}\tilde{\psi}_n = -\frac{C}{2}(\tilde{\psi}_{n+1} + \tilde{\psi}_{n-1})$$
$$+ \left[\sigma|\tilde{\psi}_n|^2 + \sum_{m\neq n}(F_{nm}|\tilde{\psi}_m|^2 + G_{nm}|\tilde{\phi}_m|^2)\right]$$
$$\times \tilde{\psi}_n - J\tilde{\phi}_n + i\kappa\tilde{\psi}_n,$$
$$i\frac{d}{dt}\tilde{\phi}_n = -\frac{C}{2}(\tilde{\phi}_{n+1} + \tilde{\phi}_{n-1})$$
$$+ \left[\sigma|\tilde{\phi}_n|^2 + \sum_{m\neq n}(F_{nm}|\tilde{\phi}_m|^2 + G_{mn}|\tilde{\psi}_m|^2)\right]$$
$$\times \tilde{\phi}_n - J\tilde{\psi}_n - i\kappa\tilde{\phi}_n. \quad (12)$$

where $\kappa > 0$ is the coefficient accounting for the gain and loss of atoms in the first and second components, respectively. The continuum limit of Eq. (12), with dominant local nonlinearity, resembles known models of nonlinear $\mathcal{PT}$-symmetric couplers, in which the $\mathcal{P}$ transformation amounts to swapping the two coupled cores, one carrying gain and the other being lossy [70–72]. In the general case of $0 < \theta < \pi/2$ considered in this work, which corresponds to the asymmetric interaction matrix G_{nm}, Eq. (12) realizes the cross-$\mathcal{PT}$ symmetry, in the sense of the cross symmetry defined as Eq. (16) below. Because the latter definition is actually tantamount to the $\mathcal{P}$ transformation along discrete coordinate n, Eq. (12) effectively defines a 2D $\mathcal{PT}$-symmetric system (cf. the definition of $\mathcal{CPT}$ symmetry proposed in Ref. [66]).

In the continuous model of the $\mathcal{PT}$-symmetric coupler with cubic intra-core nonlinearity, stationary symmetric solutions take the general form of [70,72]

$$\tilde{\psi}(x) = e^{-i\mu t}f(x)\exp[(i/2)\arcsin\kappa],$$
$$\tilde{\phi}(x) = e^{-i\mu t}f(x)\exp[-(i/2)\arcsin\kappa], \quad (13)$$

where μ is a real chemical potential of the solutions, and real $f(x)$ is a solution of the single continuous equation without the $\mathcal{PT}$ terms, for the same μ. Accordingly, a $\mathcal{PT}$-symmetric

solution of the discrete system is looked for as

$$\tilde{\psi}_n = e^{-i\mu t}f_n\exp[(i/2)\arcsin\kappa] \equiv e^{-i\mu t}\psi_n,$$
$$\tilde{\phi}_n = e^{-i\mu t}f_n\exp[-(i/2)\arcsin\kappa] \equiv e^{-i\mu t}\phi_n. \quad (14)$$

Equation (14) suggests that $\mathcal{PT}$-symmetric states exist when $\kappa < 1$, satisfying the following relations:

$$\text{Re}[\psi_n] = \text{Re}[\psi_{-n}] = \text{Re}[\phi_n] = \text{Re}[\phi_{-n}],$$
$$\text{Im}[\phi_n] = \text{Im}[\phi_n] = -\text{Im}[\phi_n] = -\text{Im}[\phi_{-n}],$$
$$|\psi_n|^2 = |\psi_{-n}|^2 = |\phi_n|^2 = |\phi_{-n}|^2, \quad (15)$$

cf. Eq. (8). In our system, Eq. (15) holds when the nonlocal cross interaction is symmetric, i.e., with a symmetric matrix G_{nm}, which is correct for the orientation angles $\theta = 0$ or $\pi/2$. As said above, in the case of asymmetric G_{nm}, i.e., for $0 < \theta < \pi/2$, the spatial symmetry is replaced by the on-site or off-site cross symmetry, i.e., discrete cross-$\mathcal{PT}$-symmetric solitons should be subject to constraints

$$\text{Re}[\psi_n] = \text{Re}[\phi_{-n}], \quad \text{Im}[\phi_n] = -\text{Im}[\phi_{-n}],$$
$$|\psi_n|^2 = |\phi_{-n}|^2, \quad (16)$$

or

$$\text{Re}[\psi_n] = \text{Re}[\phi_{1-n}], \quad \text{Im}[\phi_n] = -\text{Im}[\phi_{1-n}],$$
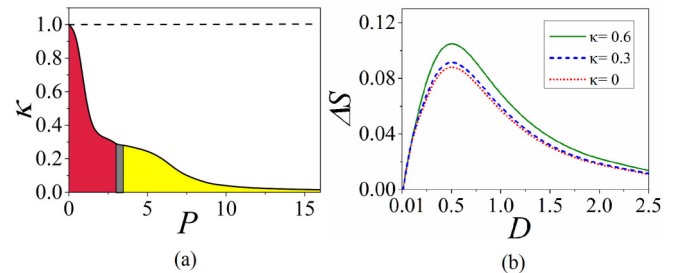$$|\psi_n|^2 = |\phi_{1-n}|^2. \quad (17)$$

FIG. 10. (a) The stability map for discrete solitons in the cross-$\mathcal{PT}$-symmetric system for $(D,\theta) = (0.4,0.196\pi)$. The red and yellow areas represents stability regions for the cross-$\mathcal{PT}$-symmetric solitons of the on- and off-site types, respectively. The intermediate gray stripe, $3 < P < 3.3$, is populated by unstable asymmetric solitons. All solutions are unstable in the white area. (b) The cross-symmetry measure (10) vs D, for the solitons of the on-site cross-$\mathcal{PT}$-symmetric type with $(P,\theta) = (1.5,0.196\pi)$, cf. Fig. 3(a) for the conservative system.
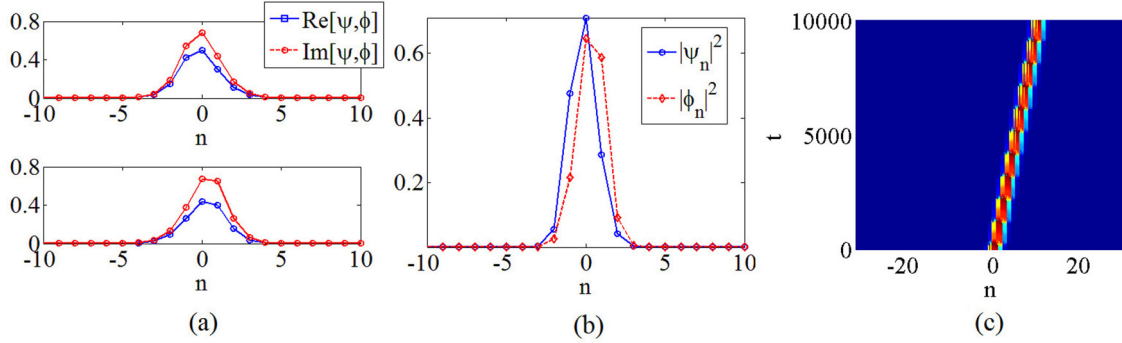
FIG. 11. A typical example of an unstable asymmetric soliton found in the cross-$\mathcal{PT}$-symmetric system for $(P,D,\theta,\kappa) = (3.15, 0.4, 0.196\pi, 0.05)$. Panels have the same meaning as in Figs. 8 and 9. (c) clearly demonstrates that the instability turns the stationary solitons into an effectively stable moving breather.

Figures 8 and 9 display several typical examples of cross-$\mathcal{PT}$-symmetric solitons of the of the on- and off-site types. Similar to their counterpart in the conservative system, the off-site cross-$\mathcal{PT}$-symmetric solitons exist, as stable states, only in a narrow area in a vicinity of $\theta = 0.196\pi$ and $D = 0.4$. Further, Fig. 10(a) displays a stability area of these two types of solitons in the (κ, P) plane for $\theta = 0.196\pi$ and $D = 0.4$. Sandwiched between the two stability areas is a narrow (gray) stripe, where asymmetric solitons of the intermediate type are found in the cross-$\mathcal{PT}$-symmetric system, see a typical example in Fig. 11. Unlike their counterparts in the conservative system, the asymmetric solitons are unstable. However, on the contrary to unstable solitons in the usual $\mathcal{PT}$-symmetric systems [64], they do not suffer a blowup, as a result of the instability development. Instead, the instability turns these solitons into robust moving breathers, as shown in Fig. 11(c)

The influence of the strength of the gain-loss coefficient on the degree of the cross symmetry, ΔS [defined by the same expression (10) as above] was studied too, as shown in Fig. 10(b), which displays $\Delta S(D)$ dependences for different fixed values of κ, at fixed $\theta = 0.196\pi$ and $P = 1.5$. It is seen that the increase of κ slightly enhances the cross-$\mathcal{PT}$

symmetry, by making ΔS somewhat larger than in the case of $\kappa = 0$.

Stable cross-$\mathcal{PT}$-symmetric solitons feature robust oscillations under the action of random perturbations, see an example displayed in Fig. 12(a). As shown in Fig. 12(b), the peak frequency of the power spectrum of the intrinsic oscillations of stable solitons of both the on-site and off-site centered types increases with the growth of the soliton's total power. Actually, it identifies the frequency of a dominant internal mode of the stable cross-$\mathcal{PT}$-symmetric solitons.

V. CONCLUSION

We have introduced the model of the chain of double-well potential traps for dipolar BEC. In the tight-binding approximation, it amounts to a system of two coupled discrete Gross-Pitaevskii equations with the long-range dipole-dipole interactions (DDIs) determined by angle θ of the orientation of the dipoles with respect to the system's axis. Except for the limit cases of $\theta = 0$ and $\theta = \pi/2$, the system, with the spatially asymmetric DDIs between the two parallel lattices, gives rise to the cross-symmetric discrete two-component solitons of two different types, on-site or off-site centered. These two families are stable, being separated by a very narrow region populated by intermediate asymmetric discrete solitons, which are stable too. Finally, we have extended the analysis by adding the $\mathcal{PT}$ symmetry to the system. In this case, stability areas for the cross-$\mathcal{PT}$-symmetric solitons of the on- and off-site-centered solitons have been identified. The corresponding intermediate asymmetric solitons are unstable, evolving into robust breathers.

It may be interesting to extend the work to the consideration of higher-order solitons, such as twisted (spatially antisymmetric [52]) ones. A challenging possibility is to introduce a two-dimensional version of the present discrete system.
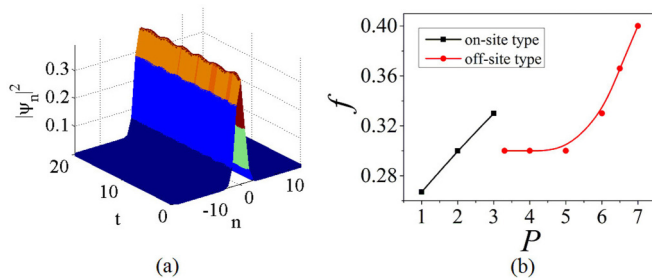

FIG. 12. (a) An example of robust oscillations of a stable cross-$\mathcal{PT}$-symmetric soliton of the on-site-centered type, excited by adding a white-noise perturbation to the initial conditions, with a 2% relative amplitude. Parameters of this soliton are $(P,D,\theta,\kappa) = (2, 0.4, 0.196\pi, 0.1)$. (b) The frequency of the intrinsic oscillations of the randomly perturbed solitons of both on-site and off-site-centered types, which corresponds to the maximum of the respective power spectrum, versus the total power of the soliton. The other parameters are $(D,\theta,\kappa) = (0.4, 0.196\pi, 0.1)$.

---

[1] A. Griesmaier, Generation of a dipolar Bose-Einstein condensate, J. Phys. B **40**, R91 (2007).

[2] T. Lahaye, C. Menotti, L. Santos, M. Lewenstein, and T. Pfau, The physics of dipolar bosonic quantum gases, Rep. Prog. Phys. **72**, 126401 (2009).

[3] M. A. Baranov, Theoretical progress in many-body physics with ultracold dipolar gases, Phys. Rep. **464**, 71 (2008).

[4] S. Giovanazzi, A. Görlitz, and T. Pfau, Tuning the Dipolar Interaction in Quantum Gases, Phys. Rev. Lett. **89**, 130401 (2002).

[5] Y. Li, J. Liu, W. Pang, and B. A. Malomed, Matter-wave solitons supported by field-induced dipole-dipole repulsion with spatially modulated strength, Phys. Rev. A **88**, 053630 (2013).

[6] L. Santos, G. V. Shlyapnikov, and M. Lewenstein, Roton-Maxon Spectrum and Stability of Trapped Dipolar Bose-Einstein Condensates, Phys. Rev. Lett. **90**, 250403 (2003); M. Klawunn, R. Nath, P. Pedri, and L. Santos, Transverse Instability of Straight Vortex Lines in Dipolar Bose-Einstein Condensates, *ibid.* **100**, 240403 (2008); R. M. Wilson, S. Ronen, J. L. Bohn, and H. Pu, Manifestations of the Roton Mode in Dipolar Bose-Einstein Condensates, *ibid.* **100**, 245302 (2008); D. Hufnagl, R. Kaltseis, V. Apaja, and R. E. Zillich, Roton-Roton Crossover in Strongly Correlated Dipolar Bose-Einstein Condensates, *ibid.* **107**, 065303 (2011); R. M. Wilson, C. Ticknor, J. L. Bohn, and E. Timmermans, Roton immiscibility in a two-component dipolar Bose gas, Phys. Rev. A **86**, 033606 (2012); L. E. Young-S. and S. K. Adhikari, Mixing, demixing, and structure formation in a binary dipolar Bose-Einstein condensate, *ibid.* **86**, 063611 (2012); A. Boudjemâa and G. V. Shlyapnikov, Two-dimensional dipolar Bose gas with the roton-maxon excitation spectrum, *ibid.* **87**, 025601 (2013); A. K. Fedorov, I. L. Kurbakov, Y. E. Shchadilova, and Yu. E. Lozovik, Two-dimensional Bose gas of tilted dipoles: Roton instability and condensate depletion, *ibid.* **90**, 043616 (2014).

[7] T. Lahaye, T. Koch, B. Fröhlich, M. Fattori, J. Metz, A. Griesmaier, S. Giovanazzi, and T. Pfau, Strong dipolar effects in a quantum ferrofluid, Nature (London) **448**, 672 (2007); H. Saito, Y. Kawaguchi, and M. Ueda, Ferrofluidity in a Two-Component Dipolar Bose-Einstein Condensate, Phys. Rev. Lett. **102**, 230403 (2009); H. Kadau, M. Schmitt, M. Wenzel, C. Wink, T. Maier, I. Ferrier-Barbut, and T. Pfau, Observing the Rosensweig instability of a quantum ferrofluid, Nature (London) **530**, 194 (2016).

[8] R. Richter and I. V. Barashenkov, Two-Dimensional Solitons on the Surface of Magnetic Fluids, Phys. Rev. Lett. **94**, 184503 (2005).

[9] R. Nath and L. Santos, Faraday patterns in two-dimensional dipolar Bose-Einstein condensates, Phys. Rev. A **81**, 033626 (2010); K. Łakomy, R. Nath, and L. Santos, Faraday patterns in coupled one-dimensional dipolar condensates, *ibid.* **86**, 023620 (2012).

[10] A. Bühler and H. P. Büchler, Supersolid phase in atomic gases with magnetic dipole interaction, Phys. Rev. A **84**, 023607 (2011); A. Maluckov, G. Gligoric, Lj. Hadžievski, B. A. Malomed, and T. Pfau, Stable Periodic Density Waves in Dipolar Bose-Einstein Condensates Trapped in Optical Lattices, Phys. Rev. Lett. **108**, 140402 (2012); Z.-K. Lu, Y. Li, D. S. Petrov, and G. V. Shlyapnikov, Stable Dilute Supersolid of Two-Dimensional Dipolar Bosons, *ibid.* **115**, 075303 (2015).

[11] C. Ticknor, R. M. Wilson, and J. L. Bohn, Anisotropic Superfluidity in a Dipolar Bose Gas, Phys. Rev. Lett. **106**, 065301 (2011); X.-F. Zhang, T. Wang, S. Eggert, and A. Pelster, Tunable anisotropic superfluidity in an optical kagome superlattice, Phys. Rev. B **92**, 014512 (2015); A. Boudjemâa, Superfluidity and Bose-Einstein condensation in a dipolar Bose gas with weak disorder, J. Low Temp. Phys. **180**, 377 (2015); Dipolar Bose gas in a weak isotropic speckle disorder, Phys. Rev. A **91**, 053619 (2015); A. A. Wood, B. H. J. McKellar, and A. M. Martin, Persistent Superfluid Flow Arising from the He-Mckellar-Wilkens Effect in Molecular Dipolar Condensates, Phys. Rev. Lett. **116**, 250403 (2016).

[12] P. M. Lushnikov, Collapse of Bose-Einstein condensates with dipole-dipole interactions, Phys. Rev. A **66**, 051601(R) (2002); D. C. E. Bortolotti, S. Ronen, J. L. Bohn, and D. Blume, Scattering Length Instability in Dipolar Bose-Einstein Condensates, Phys. Rev. Lett. **97**, 160402 (2006); C. Ticknor, N. G. Parker, A. Melatos, S. L. Cornish, D. H. J. O'Dell, and A. M. Martin, Collapse times of dipolar Bose-Einstein condensates, Phys. Rev. A **78**, 061607(R) (2008); T. Lahaye, J. Metz, B. Fröhlich, T. Koch, M. Meister, A. Griesmaier, T. Pfau, H. Saito, Y. Kawaguchi, and M. Ueda, *d*-Wave Collapse and Explosion of a Dipolar Bose-Einstein Condensate, Phys. Rev. Lett. **101**, 080401 (2008).

[13] I. Ferrier-Barbut, H. Kadau, M. Schmitt, M. Wenzel, and T. Pfau, Observation of Quantum Droplets in a Strongly Dipolar Bose Gas, Phys. Rev. Lett. **116**, 215301 (2016); K.-T. Xi and H. Saito, Droplet formation in a Bose-Einstein condensate with strong dipole-dipole interaction, Phys. Rev. A **93**, 011604(R) (2016); F. Wächtler and L. Santos, Quantum filaments in dipolar Bose-Einstein condensates, *ibid.* **93**, 061603(R) (2016); D. Baillie, R. M. Wilson, R. N. Bisset, and P. B. Blakie, Self-bound dipolar droplet: A localized matter wave in free space, *ibid.* **94**, 021602(R) (2016); A. Macia, J. Sánchez-Baena, J. Boronat, and F. Mazzanti, Droplets of Trapped Quantum Dipolar Bosons, Phys. Rev. Lett. **117**, 205301 (2016).

[14] Y. Kawaguchi, H. Saito, and M. Ueda, Einstein-De Haas Effect in Dipolar Bose-Einstein Condensates, Phys. Rev. Lett. **96**, 080405 (2006); Y. Deng, J. Cheng, H. Jing, C.-P. Sun, and S. Yi, Spin-Orbit-Coupled Dipolar Bose-Einstein Condensates, *ibid.* **108**, 125301 (2012).

[15] M. Klawunn and L. Santos, Hybrid multisite excitations in dipolar condensates in optical lattices, Phys. Rev. A **80**, 013611 (2009).

[16] S. Müller, J. Billy, E. A. L. Henn, H. Kadau, A. Griesmaier, M. Jona-Lasinio, L. Santos, and T. Pfau, Stability of a dipolar Bose-Einstein condensate in a one-dimensional lattice, Phys. Rev. A **84**, 053601 (2011).

[17] R. M. Wilson and J. L. Bohn, Emergent structure in a dipolar Bose gas in a one-dimensional lattice, Phys. Rev. A **83**, 023623 (2011).

[18] K. Gawryluk, K. Bongs, and M. Brewczyk, How to Observe Dipolar Effects in Spinor Bose-Einstein Condensates, Phys. Rev. Lett. **106**, 140403 (2011); U. R. Fischer, Stability of quasi-two-dimensional Bose-Einstein condensates with dominant dipole-dipole interactions, Phys. Rev. A **73**, 031602(R) (2006).

[19] W. Królikowski, O. Bang, N. I. Nikolov, D. Neshev, J. Wyller, J. J. Rasmussen, and D. Edmundson, Modulational instability, solitons and beam propagation in spatially nonlocal nonlinear media, J. Opt. B: Quantum Semiclass. Opt. **6**, S288 (2004); M. Peccianti and G. Assanto, Nematicons, Phys. Rep. **516**, 147 (2012).

[20] W. Królikowski and O. Bang, Solitons in nonlocal nonlinear media: Exact solutions, Phys. Rev. E **63**, 016610 (2000); S. Skupin, O. Bang, D. Edmundson, and W. Królikowski, Stability of two-dimensional spatial solitons in nonlocal nonlinear media, ibid. **73**, 066603 (2006).

[21] P. Pedri and L. Santos, Two-Dimensional Bright Solitons in Dipolar Bose-Einstein Condensates, Phys. Rev. Lett. **95**, 200404 (2005); I. Tikhonenkov, B. A. Malomed, and A. Vardi, Anisotropic Solitons in Dipolar Bose-Einstein Condensates, ibid. **100**, 090406 (2008); J. Cuevas, B. A. Malomed, P. G. Kevrekidis, and D. J. Frantzeskakis, Solitons in quasi-one-dimensional Bose-Einstein condensates with competing dipolar and local interactions, Phys. Rev. A **79**, 053608 (2009); P. Köberle, D. Zajec, G. Wunner, and B. A. Malomed, Creating two-dimensional bright solitons in dipolar Bose-Einstein condensates, ibid. **85**, 023630 (2012); F. Kh. Abdullaev, A. Gammal, B. A. Malomed, and L. Tomio, Bright solitons in quasi-one dimensional dipolar condensates with spatially modulated interactions, ibid. **87**, 063621 (2013); M. Raghunandan, C. Mishra, K. Łakomy, P. Pedri, L. Santos, and R. Nath, Two-dimensional bright solitons in dipolar Bose-Einstein condensates with titled dipoles, ibid. **92**, 013637 (2015); S. K. Adhikari and L. E. Young-S, Statics and dynamics of a binary dipolar Bose–Einstein condensate soliton, J. Phys. B **47**, 015302 (2014).

[22] R. Nath, P. Pedri, and L. Santos, Stability of Dark Solitons in Three Dimensional Dipolar Bose-Einstein Condensates, Phys. Rev. Lett. **101**, 210402 (2008); T. Bland, M. J. Edmonds, N. P. Proukakis, A. M. Martin, D. H. J. O'Dell, and N. G. Parker, Controllable nonlocal interactions between dark solitons in dipolar condensates, Phys. Rev. A **92**, 063601 (2015); K. Pawłowski and K. Rzążewski, Dipolar dark solitons, New J. Phys. **17**, 105006 (2015); M. J. Edmonds, T. Bland, D. H. J. O'Dell, and N. G. Parker, Exploring the stability and dynamics of dipolar matter-wave dark solitons, Phys. Rev. A **93**, 063617 (2016).

[23] V. M. Lashkin, Two-dimensional nonlocal vortices, multipole solitons, and rotating multisolitons in dipolar Bose-

Einstein condensates, Phys. Rev. A **75**, 043607 (2007); I. Tikhonenkov, B. A. Malomed, and A. Vardi, Vortex solitons in dipolar Bose-Einstein condensates, ibid. **78**, 043614 (2008).

[24] G. Gligorić, A. Maluckov, L. Hadžievski, and B. A. Malomed, Bright solitons in the one-dimensional discrete Gross-Pitaevskii equation with dipole-dipole interactions, Phys. Rev. A **78**, 063615 (2008); G. Gligorić, A. Maluckov, M. Stepić, L. Hadžievski, and B. A. Malomed, Two-dimensional discrete solitons in dipolar Bose-Einstein condensates, ibid. **81**, 013633 (2010); H. Chen, Y. Liu, Q. Zhang, Y. Shi, W. Pang, and Y. Li, Dipolar matter-wave solitons in two-dimensional anisotropic discrete lattices, ibid. **93**, 053608 (2016).

[25] Y. Xu, Y. Zhang, and C. Zhang, Bright solitons in a two-dimensional spin-orbit-coupled dipolar Bose-Einstein condensate, Phys. Rev. A **92**, 013633 (2015); X. Jiang, Z. Fan, Z. Chen, W. Pang, Y. Li, and B. A. Malomed, Two-dimensional solitons in dipolar Bose-Einstein condensates with spin-orbit-coupling, ibid. **93**, 023633 (2016).

[26] B. B. Baizakov, F. Kh. Abdullaev, B. A. Malomed, and M. Salerno, Solitons in Tonks-Girardeau gas with dipolar interactions, J. Phys. B **42**, 175302 (2009).

[27] Edited by B. A. Malomed, *Spontaneous Symmetry Breaking, Self-Trapping, and Josephson Oscillations* (Springer, Berlin, 2013).

[28] B. A. Malomed, Spontaneous symmetry breaking in nonlinear systems: An overview and a simple model, in *Nonlinear Dynamics: Materials, Theory and Experiments*, edited by M. Tlidi and M. Clerc, Springer Proceedings in Physics Vol. 173 (Springer, Berlin, 2016), pp. 97–112.

[29] S. Trillo, S. Wabnitz, E. M. Wright, and G. I. Stegeman, Soliton switching in fiber nonlinear directional couplers, Opt. Lett. **13**, 672 (1988).

[30] S. R. Friberg, A. M. Weiner, Y. Silberberg, B. G. Sfez, and P. S. Smith, Femtosecond switching in a dual-core-fiber nonlinear coupler, Opt. Lett. **13**, 904 (1988).

[31] F. Kh. Abdullaev, R. M. Abrarov, and S. A. Darmanyan, Dynamics of solitons in coupled optical fibers, Opt. Lett. **14**, 131 (1989).

[32] S. Trillo, S. Wabnitz, E. M. Wright, G. I. Stegeman, Polarized soliton instability and branching in birefringent fibers, Opt. Commun. **70**, 166 (1989).

[33] C. Pare and M. Fłorjańczyk, Approximate model of soliton dynamics in all-optical couplers, Phys. Rev. A **41**, 6287 (1990).

[34] A. I. Maimistov, Propagation of a light pulse in nonlinear tunnel-coupled optical waveguides, Sov. J. Quantum Electron. **21**, 687 (1991).

[35] M. Romagnoli, S. Trillo, and S. Wabnitz, Soliton switching in nonlinear couplers, Opt. Quantum Electron. **24**, S1237 (1992).

[36] N. Akhmediev and A. Ankiewicz, Novel Soliton States and Bifurcation Phenomena in Nonlinear Fiber Couplers, Phys. Rev. Lett. **70**, 2395 (1993).

[37] P. L. Chu, B. A. Malomed, and G. D. Peng, Soliton switching and propagation in nonlinear fiber couplers: Analytical results, J. Opt. Soc. Am. B **10**, 1379 (1993).

[38] J. M. Soto-Crespo and N. Akhmediev, Stability of the soliton states in a nonlinear fiber coupler, Phys. Rev. E **48**, 4710 (1993).

[39] W. C. K. Mak, B. A. Malomed, and P. L. Chu, Solitary waves in coupled nonlinear waveguides with Bragg gratings, J. Opt. Soc. Am. B **15**, 1685 (1998).

[40] M. Matuszewski, B. A. Malomed, and M. Trippenbach, Spontaneous symmetry breaking of solitons trapped in a double-channel potential, Phys. Rev. A **75**, 063621 (2007).

[41] Y. J. Tsofe and B. A. Malomed, Quasisymmetric and asymmetric gap solitons in linearly coupled Bragg gratings with a phase shift, Phys. Rev. E **75**, 056603 (2007).

[42] S. Ha, A. A. Sukhorukov, and Y. S. Kivshar, Slow-light switching in nonlinear Bragg-grating couplers, Opt. Lett. **32**, 1429 (2007).

[43] S. Ha and A. A. Sukhorukov, Nonlinear switching and reshaping of slow-light pulses in Bragg-grating couplers, J. Opt. Soc. Am. B **25**, C15 (2008).

[44] S. K. Adhikari and B. A. Malomed, Two-component gap solitons with linear interconversion, Phys. Rev. A **79**, 015602 (2009).

[45] H. Sakaguchi and B. A. Malomed, Symmetry breaking of solitons in two-component Gross-Pitaevskii equations, Phys. Rev. E **83**, 036608 (2011).

[46] Y. Li, B. A. Malomed, M. Feng, and J. Zhou, Double symmetry breaking of solitons in one-dimensional virtual photonic crystals, Phys. Rev. A **83**, 053832 (2011).

[47] G. Herring, P. G. Kevrekidis, B. A. Malomed, R. Carretero-González, and D. J. Frantzeskakis, Symmetry breaking in linearly coupled dynamical lattices, Phys. Rev. E **76**, 066606 (2007).

[48] X. Shi, B. A. Malomed, F. Ye, and X. Chen, Symmetric and asymmetric solitons in a nonlocal nonlinear coupler, Phys. Rev. A **85**, 053839 (2012).

[49] Y. Li, J. Liu, W. Pang, and B. A. Malomed, Symmetry breaking in dipolar matter-wave solitons in dual-core couplers, Phys. Rev. A **87**, 013604 (2013).

[50] V. A. Brazhnyi and V. V. Konotop, Theory of nonlinear matter waves in optical lattices, Mod. Phys. Lett. B **18**, 627 (2004); O. Morsch and M. Oberthaler, Dynamics of Bose-Einstein condensates in optical lattices, Rev. Mod. Phys. **78**, 179 (2006).

[51] A. Trombettoni and A. Smerzi, Discrete Solitons and Breathers with Dilute Bose-Einstein Condensates, Phys. Rev. Lett. **86**, 2353 (2001); F. Kh. Abdullaev, B. B. Baizakov, S. A. Darmanyan, V. V. Konotop, and M. Salerno, Nonlinear excitations in arrays of Bose-Einstein condensates, Phys. Rev. A **64**, 043606 (2001); G. L. Alfimov, P. G. Kevrekidis, V. V. Konotop, and M. Salerno, Wannier functions analysis of the nonlinear Schrödinger equation with a periodic potential, Phys. Rev. E **66**, 046608 (2002); R. Carretero-González and K. Promislow, Localized breathing oscillations of Bose-Einstein condensates in periodic traps, Phys. Rev. A **66**, 033610 (2002).

[52] P. G. Kevrekidis, *The Discrete Nonlinear Schrö dinger Equation: Mathematical Analysis, Numerical Computations, and Physical Perspectives* (Springer, Berlin, 2009).

[53] Y. Li, W. Pang, J. Xu, C. Lee, B. A. Malomed, and L. Santos, Long-range transverse Ising model built with dipolar condensates in two-well arrays, New J. Phys. **19**, 013030 (2017).

[54] B. A. Malomed and M. I. Weinstein, Soliton dynamics in the discrete nonlinear Schrödinger equation, Phys. Lett. A **220**, 91 (1996); D. J. Kaup, Variational solutions for the discrete nonlinear Schrödinger equation, Math. Comp. Sim. **69**, 322 (2005).

[55] M. L. Chiofalo, S. Succi, and M. P. Tosi, Ground state of trapped interacting Bose-Einstein condensates by an explicit imaginary-time algorithm, Phys. Rev. E **62**, 7438 (2000).

[56] J. Yang and T. I. Lakoba, Accelerated imaginary-time evolution methods for the computation of solitary waves, Stud. Appl. Math. **120**, 265 (2008).

[57] J. Yang and T. I. Lakoba, Universally-convergent squared-operator iteration methods for solitary waves in general nonlinear wave equations, Stud. Appl. Math. **118**, 153 (2007).

[58] N. G. Vakhitov and A. A. Kolokolov, Stationary solutions of the wave equation in the medium with nonlinearity saturation, Radiophys. Quantum Electron. **16**, 783 (1973); L. Bergé, Wave collapse in physics: principles and applications to light and plasma waves, Phys. Rep. **303**, 259 (1998); E. A. Kuznetsov and F. Dias, Bifurcations of solitons and their stability, *ibid.* **507**, 43 (2011).

[59] B. A. Malomed, D. J. Kaup, and R. A. Van Gorder, Unstaggered-staggered solitons in two-component discrete nonlinear Schrö dinger lattices, Phys. Rev. E **85**, 026604 (2012).

[60] C. Kollath, J. S. Meyer, and T. Giamarchi, Dipolar Bosons in a Planar Array of One-Dimensional Tubes, Phys. Rev. Lett. **100**, 130403 (2008).

[61] B. A. Malomed, A. A. Nepomnyashchy, and M. I. Tribelsky, Domain boundaries in convection patterns, Phys. Rev. A **42**, 7244 (1990).

[62] C. M. Bender and S. Boettcher, Real Spectra in Non-Hermitian Hamiltonians Having $\mathcal{PT}$ Symmetry, Phys. Rev. Lett. **80**, 5243 (1998); C. M. Bender, Making sense of non-Hermitian Hamiltonians, Rep. Prog. Phys. **70**, 947 (2007).

[63] A. Ruschhaupt, F. Delgado, and J. G. Muga, Physical realization of $\mathcal{PT}$-symmetric potential scattering in a planar slab waveguide, J. Phys. A: Math. Gen. **38**, L171 (2005); R. El-Ganainy, K. G. Makris, D. N. Christodoulides, and Z. H. Musslimani, Theory of coupled optical $\mathcal{PT}$-symmetric structures, Opt. Lett. **32**, 2632 (2007); M. V. Berry, Optical lattices with $\mathcal{PT}$ symmetry are not transparent, J. Phys. A: Math. Theor. **41**, 244007 (2008); S. Klaiman, U. Günther, and N. Moiseyev, Visualization of Branch Points in $\mathcal{PT}$-Symmetric Waveguides, Phys. Rev. Lett. **101**, 080402 (2008); S. Longhi, Bloch Oscillations in Complex Crystals with $\mathcal{PT}$ Symmetry, *ibid.* **103**, 123601 (2009).

[64] K. G. Makris, R. El-Ganainy, D. N. Christodoulides, and Z. H. Musslimani, $\mathcal{PT}$ symmetric periodic optical potentials, Int. J. Theor. Phys. **50**, 1019 (2011); S. V. Suchkov, A. A. Sukhorukov, J. Huang, S. V. Dmitriev, C. Lee, and Y. S. Kivshar, Nonlinear switching and solitons in $\mathcal{PT}$-symmetric photonic systems, Laser Photonics Rev. **10**, 177 (2016).

[65] D. Haag, D. Dast, A. Löhle, H. Cartarius, J. Main, and G. Wunner, Nonlinear quantum dynamics in a $\mathcal{PT}$-symmetric double well, Phys. Rev. A **89**, 023601 (2014).

[66] Y. V. Kartashov, V. V. Konotop, and D. A. Zezyulin, $\mathcal{CPT}$-symmetric spin-orbit–coupled condensate, Europhys. Lett. **107**, 50002 (2014).

[67] V. V. Konotop, J. Yang, and D. A. Zezyulin, Nonlinear waves in $\mathcal{PT}$-symmetric systems, Rev. Mod. Phys. **88**, 035002 (2016).

[68] A. Boudjemâa, Bose polaronic soliton-molecule and vector solitons in $\mathcal{PT}$-symmetric potential, Comm. Nonlin. Sci. Num. Sim. **48**, 376 (2017).

[69] R. Fortanier, D. Dast, D. Haag, H. Cartarius, J. Main, G. Wunner, and R. Gutöhrlein, Dipolar Bose-Einstein condensates in a $\mathcal{PT}$-symmetric double-well potential, Phys. Rev. A **89**, 063608 (2014).

[70] R. Driben and B. A. Malomed, Stability of solitons in parity-time-symmetric couplers, Opt. Lett. **36**, 4323 (2011).

[71] F. Kh. Abdullaev, V. V. Konotop, M. Øgren, and M. P. Sørensen, Zeno effect and switching of solitons in nonlinear couplers, Opt. Lett. **36**, 4566 (2011).

[72] N. V. Alexeeva, I. V. Barashenkov, A. A. Sukhorukov, and Y. S. Kivshar, Optical solitons in $\mathcal{PT}$-symmetric nonlinear couplers with gain and loss, Phys. Rev. A **85**, 063837 (2012).